ELSEVIER

Colloids and Surfaces
A: Physicochemical and Engineering Aspects 131 (1998) 109–118

COLLOIDS AND SURFACES A

Ultrafiltration of very dilute colloidal mixtures

S.S. Madaeni

Chemical Engineering Department, Razi University, Kermanshah, Iran

Received 1 July 1996; accepted 23 February 1997

Abstract

The ultrafiltration behaviour of very dilute (ca. 10 ppm) mixtures of gold (50 nm) and latex (1 μm) colloidal suspensions has been investigated in terms of transmembrane pressure and pH in a batch cell with and without stirring. The hydrophobic PM30 and the hydrophilic XM300 membranes were used as ultrafilters.

Both membranes gave higher flux and lower retention in the absence of stirring and increasing ΔP. For the PM30 membrane, increasing pH caused higher flux. For both types of membrane, a lower pressure produced a slower flux decline, lower solute resistance and higher retention. The PM30 membranes showed better performance (complete retention, slower flux decline and lower solute resistance) than the XM300 membranes due to the differences in membrane pore size and material. Pore blocking is more likely in the case of the XM300 membrane with its larger molecular weight cut-off.

The dominant mechanism was cake formation after initial pore plugging. The estimated cake specific resistance showed a small increase with pressure. The cake porosity was smaller than the reported porosity for the random packing of a binary mixture due to the effect of applied pressure.

These studies have shown that membrane filtration of dilute suspensions is a complex process. Clearly, the deposition on and within the membrane, and within the cake will be dependent on a number of parameters, including membrane type, relative particle size, species concentrations, particle charges (dependent on pH and ionic environment) and flux (dependent on pressure). The performance also varies with time. © 1998 Elsevier Science B.V.

Keywords: Ultrafiltration; Membrane; Colloids; Dilute; Gold; Latex

1. Introduction

In many practical situations, for instance wastewater treatment, two or more colloids are mixed, so the separation of a mixture of colloidal particles from an aqueous solution is of considerable importance, scientifically and industrially. Ultrafiltration of very dilute suspensions has application in ultrapure water production [1,2], water purification [3,4], virus recovery from tap water [5] or domestic effluent [6].

It has been shown [7] that the membrane filtration of dilute suspensions is sensitive to solution conditions. The effects of the presence of larger (micrometre-sized) particles on the microfiltration and ultrafiltration of dilute fine colloids are of interest.

In previous work [8], microfiltration of dilute colloidal mixtures was characterised. In this article the ultrafiltration of very dilute colloidal mixtures as a function of stirring, transmembrane pressure and pH has been investigated.

2. Experimental

2.1. Membranes

Amicon PM30 (MWCO = 30 kDa) and XM300 (MWCO = 300 kDa) membranes were used as

PII S0927-7757(97)00081-2

ultrafilters. Details of the membranes are given in Table 1. Membranes were prepared for use according to the information provided by the manufacturer.

2.2. Colloidal gold particles

Gold sol was prepared according to the method of Turkevich et al. [9] and Frens [10] by reduction of aqueous gold(III) using citrate ions. Details have been explained elsewhere [8]. For the experiments the sol (50 mg l^{-1} Au, pH = 3.3) was diluted fivefold (10 mg l^{-1} Au, pH = 4.0) with distilled water immediately before the experiments. Each set of experiments was carried out within a few days after colloidal gold preparation to avoid any difference in the sol particles due to aging. The gold sol particles had a slightly spheroidal shape with a mean diameter of 53.5 nm (standard deviation 23.7). For measuring the zeta potential of colloids a laser-based multiangle particle electrophoresis analyser, Delsa 440 (Coulter Scientific Instruments), was used. The Delsa 440 combines electrophoresis or the movement of the charged particles in an applied electric field and laser Doppler velocimetry that measures the speed of particles by analysing the Doppler shifts of scattered light. In the Delsa 440, Smoluchowski's mobility equation is used to change the mobility into the zeta potential. The zeta potential of Au sol was measured as −50 mV at pH = 4.

Table 1
Specifications of membranes

	PM30X	M300
Manufacturer	Amicon	Amicon
Material	Polysulphone	Dynel[a]
Hydrophobicity	Hydrophobic	Hydrophilic
MW cut-off (kDa)	30	300
Water flux[b] ($l\,m^{-2}\,h^{-1}$)	640–1130	1240–1600
Permeability (10^9 m $Pa^{-1}\,s^{-1}$)	1.7–3.1	3.4–4.4
Membrane resistance (10^{11} m^{-1})	3.5–4.0	2.3–2.9

[a] Poly co(acrylonitrile–vinyl chloride).
[b] $\Delta P = 100$ kPa.

2.3. Polystyrene latex particles

Polystyrene latex beads (Cat. No. LB-11) were obtained from Sigma Chemical Company. Transmission electron microscope (TEM) micrographs of polystyrene particles showed that they were spherical with a diameter of 1 μm. Reported particle diameter by the manufacturer is 1.020 μm (standard deviation < 0.004 μm). The zeta potential of latex was measured as −60 mV at pH = 4.

2.4. Filtration procedure

All experiments were carried out in a 110 ml capacity batch cell, with a membrane area of 15.2 cm^2. The specifications of the cell have been explained elsewhere [8]. The experiments started after 100 ml of a mixture of gold and latex colloids (10 mg l^{-1} Au and 10 mg l^{-1} latex) was poured into the cell which was quickly pressurised by nitrogen gas. The feed solution was fed continuously from a feed reservoir connected to the cell to replenish the permeate. For stirred experiments the magnetic stirrer was started with a stirring speed of 400 rev min^{-1} prior to the filtration. The experiments were carried out at ambient temperature (24 ± 1°C). The flux was measured gravimetrically with a Mettler PJ 6000 electronic balance by continuously weighing the permeate. The retention of gold particles was determined by $R(\%) = 100[1 - (C_p/C_b)]$, where C_p and C_b are absorbances of gold sol at 530 nm for the permeate and bulk respectively. A plot of the absorbances for the gold sol in different concentrations showed a straight line with a correlation coefficient of 1.000.

2.5. Electron microscopy of membranes

For viewing the membrane surface, an Hitachi S-900 field emission scanning electron microscope (SEM) operating at 2 kV and for observation of membrane cross-sections an Hitachi H-7000 TEM operating at 75 kV were used. The details of electron microscopy can be found elsewhere [8].

3. Results and discussion

3.1. Effect of membrane type

The XM300 membranes with 300 kDa molecular weight cut-off showed initially lower retention (Fig. 1) than the PM30 membranes (MWCO = 30 kDa) but within 30 min the retention was similar and essentially complete. The XM300 membranes (Fig. 2) did not show much higher flux than the PM30 membrane (in some cases even lower flux). This performance can be explained by pore blocking, which is more likely in the case of the partially permeable XM300 membrane. For the XM300 membranes (with a mean pore diameter of 8.6 nm and maximum pore width of 47.6 nm [11]) the particles have more chance to plug the membrane pores than the PM30 membranes (mean pore diameter of 4 nm and a maximum pore width of 18.3 nm [11]). The plugging results in lower flux for the XM300 membrane. Another factor is the difference in membrane material. The polymer that is used to make the membrane affects the retention [12,13].

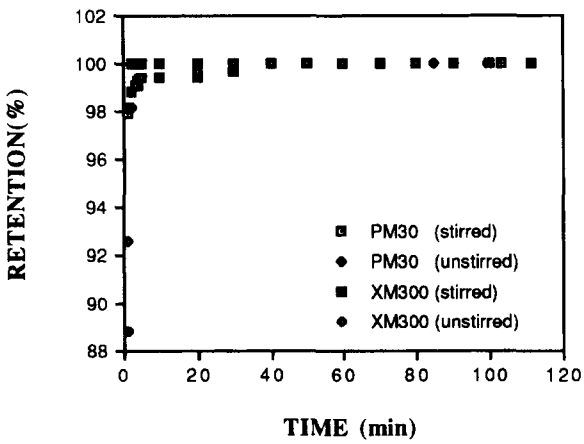

Fig. 1. Retention profiles of a mixture of Au sol and latex using PM30 and XM300 membranes under stirred (400 rev min^{-1}) and unstirred conditions (10 mg l^{-1} Au, 10 mg l^{-1} latex, 100 kPa, pH = 4).

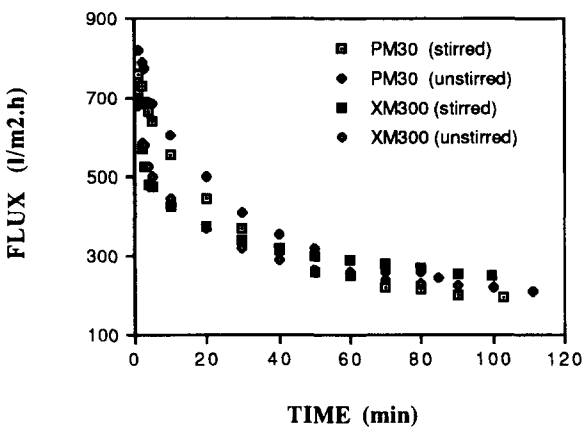

Fig. 2. Flux profiles of a mixture of Au sol and latex using PM30 and XM300 membranes under stirred (400 rev min^{-1}) and unstirred conditions (10 mg l^{-1} Au, 10 mg l^{-1} latex, 100 kPa, pH = 4).

3.2. Transmembrane pressure

By increasing the applied transmembrane pressure, the flux, flux loss and solute resistances were increased (Tables 2 and 3). Flux decline was due to the formation of a sticky cake layer. This layer could not be removed by washing and remained stable on the surface of the membrane. Initial water flux J_{wi} (before the experiment) and final water flux J_{wf} (after the experiment) were measured. A typical ratio of J_{wf} to J_{wi} after the passage

Table 2
Effect of transmembrane pressure on solute resistance R_s and flux loss[a] J_{loss} of a mixture of Au sol and latex using PM30 membrane at 400 rev min^{-1} and pH = 4 after filtering 800 ml of solution

ΔP (kPa)	J_{loss} (%)	R_s (10^{11} m^{-1})
50	56	5.7
100	74	14.9
200	79	20.0

Initial flux is the flux after 1 min.
[a] Flux loss(%) = [ΔJ(initial − final)/initial flux] × 100.

Table 3
Effect of transmembrane pressure on solute resistance R_s and flux loss J_{loss} of a mixture of Au sol and latex using XM300 membrane at 400 rev min^{-1} and pH = 4 after filtering 800 ml of solution

ΔP (kPa)	J_{loss} (%)	R_s (10^{11} m^{-1})
50	61	10.0
100	64	10.9
200	68	15.8

of 800 ml of the feed through the PM30 membrane at 100 kPa was 0.21. This observation shows that flux decline is caused by fouling.

Retention of gold particles was decreased by increasing ΔP for the case of the XM300 membrane (Fig. 3) and was complete for PM30 membrane at all pressures. Lower retention at higher ΔP is typical in UF and can be explained by a higher concentration at the membrane surface due to increased polarisation giving a higher concentration in the permeate. For both membranes, lower pressure produced slower flux decline, lower solute resistance and higher retention (less initial transmission).

3.3. Effect of pH

Increasing pH causes slightly higher flux (Fig. 4). Rejection was complete in both cases. The isoelectric points of the latex and gold particles are 2.3 and 2.9 respectively. Therefore, the particles gain extra charge upon increasing the pH from 4 to 7. This extra charge causes more porosity in the cake, leading to reduction in the resistance [14]. Membrane charge can also play a role. The isoelectric point of the PM30 membranes is 3 [15]. They obtain more negative charge when pH is increased [16]. This results in lower adsorption of the negatively charged colloidal particles. Less adsorption means lower resistance and higher flux.

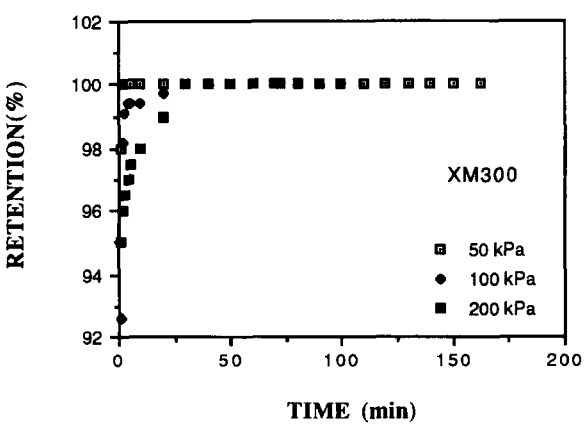

Fig. 3. Retention profiles of mixtures of Au sol and latex using XM300 membrane as a function of transmembrane pressure (10 mg l^{-1} Au, 10 mg l^{-1} latex, 400 rev min^{-1}, pH = 4).

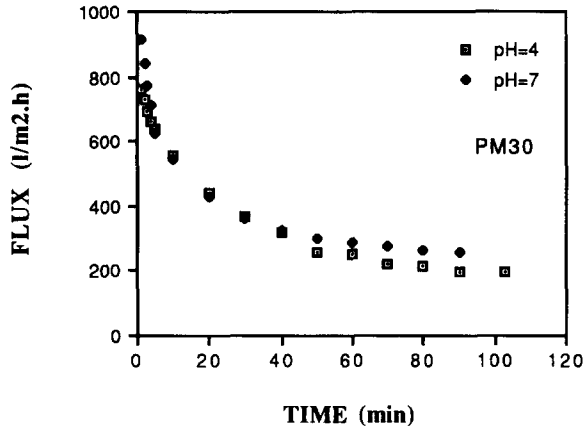

Fig. 4. Flux profiles of a mixture of Au sol and latex as a function of pH using PM30 membranes (10 mg l^{-1} Au, 10 mg l^{-1} latex, 400 rev min^{-1}).

3.4. Filtration mechanism

It is of interest to compare the unstirred data (permeate volume V, and time t) using the blocking laws [17]. For a mechanism of pore blocking the plot of $\exp(t)$ vs. V should be linear, for cake deposition control t/V vs. V should be linear, and for internal pore closure t/V vs. t should be linear.

The plots of t/V vs. V for both PM30 and XM300 membranes (Fig. 5) indicate that cake formation is the dominant mechanism. As the filtration starts, both gold and latex particles that are larger than the pores of the membrane settle

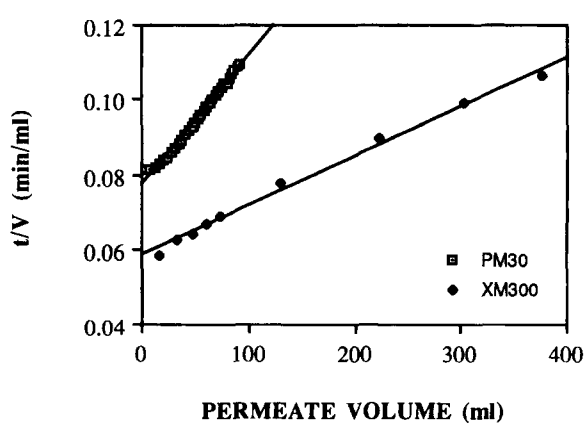

Fig. 5. Determination of filtration mechanism of a mixture of Au sol and latex using PM30 and XM300 membranes (10 mg l^{-1} Au, 10 mg l^{-1} latex, 100 kPa, unstirred, pH = 4).

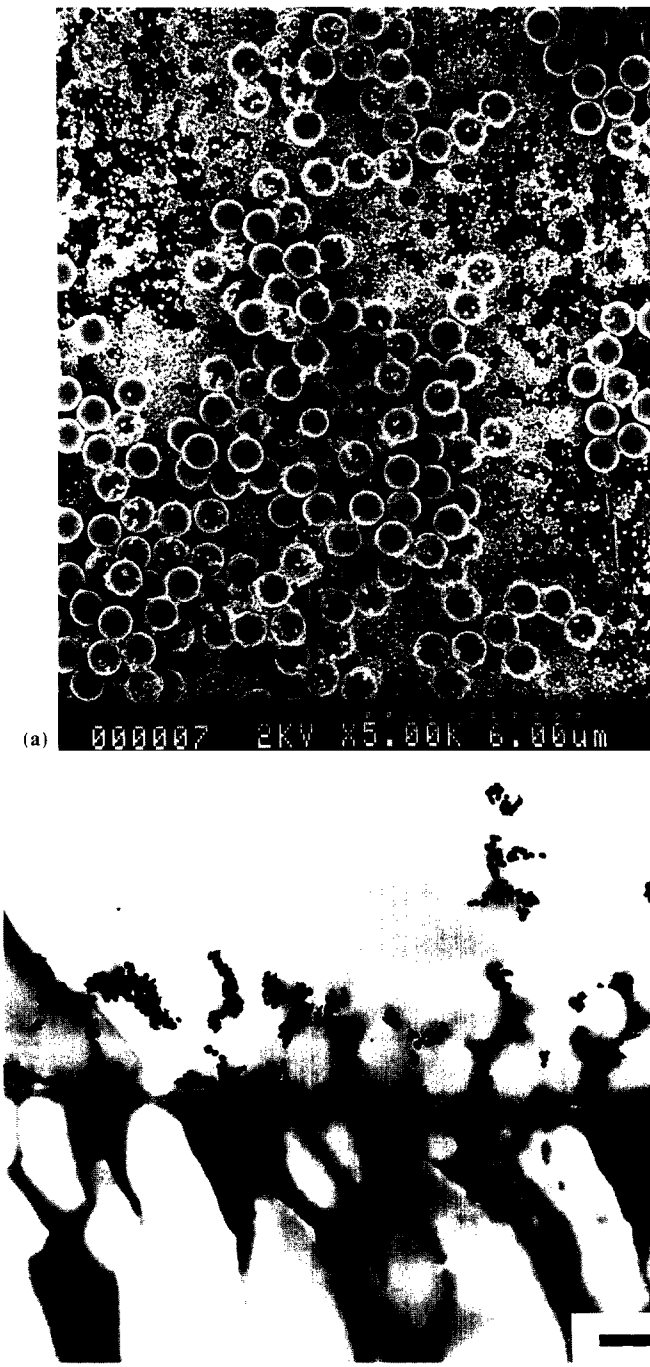

Fig. 6. (a) SEM and (b) TEM micrographs of PM30 membrane after filtering 100 ml of a mixture of Au sol and latex (10 mg l^{-1} Au, 10 mg l^{-1} latex, 100 kPa, unstirred, pH = 4).

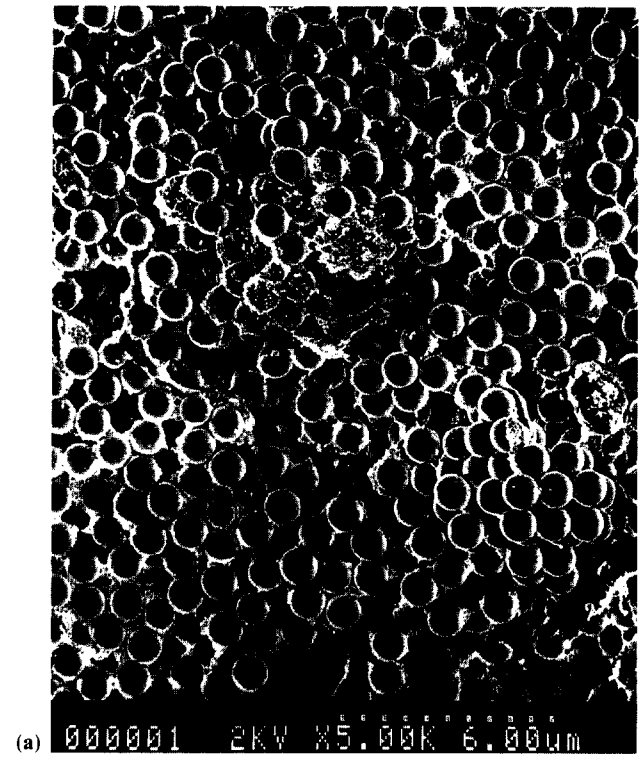

Fig. 7. (a) SEM and (b) TEM micrographs of XM300 membrane after filtering 800 ml of a mixture of Au sol and latex (10 mg Au, 10 mg l^{-1} latex, 100 kPa, 400 rev min^{-1}, pH = 4).

Table 4
Specific resistances of the cake of Au sol α_{Au}, latex α_{latex} and a mixture of Au sol and latex α_{mix} as a function of transmembrane pressure

ΔP (kPa)	α_{Au} (10^{13} m kg^{-1})	α_{latex} (10^{13} m kg^{-1})	α_{mix} (10^{13} m kg^{-1})
50	1.0	0.35	13.5
100	1.1	0.40	20.3
200	1.2	0.50	22.3
300	1.3	0.54	25.6

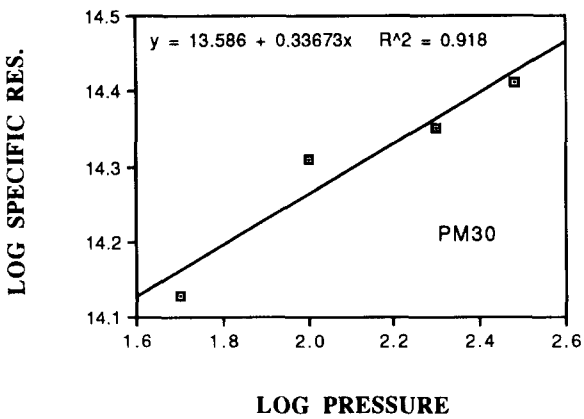

Fig. 8. Specific resistance of a mixture of Au sol and latex cake as a function of transmembrane pressure using PM30 membrane (10 mg l^{-1} Au, 10 mg l^{-1} latex, 100 kPa, unstirred, pH = 4).

on the membrane surface (Fig. 6). The cake is progressively thickened and more layers are formed (Fig. 7).

In the case of the XM300 membrane, the initial deviation from linearity suggests initial pore plugging. The large pores in the size distribution of this membrane can be blocked by gold particles. In the case of the XM300 membranes, with mean pore diameter of 8.6 nm and maximum pore width of 47.6 nm [11], the particles have more chance to plug the membrane pores than the PM30 membranes (mean pore diameter of 4 nm and maximum pore width of 18.3 nm [11]). However, if membrane resistance is much less than the cake resistance then t/V vs. V is linear [18], which is not true at the beginning of the filtration while the cake is forming. The same trend for the t/V vs. V curve was observed by Murase et al. [19].

Table 5
Porosity of the cake of Au sol ϵ_{Au}, latex ϵ_{latex} and a mixture of Au sol and latex ϵ_{mix} as a function of transmembrane pressure

ΔP (kPa)	ϵ_{Au}	ϵ_{latex}	ϵ_{mix}
50	0.55	0.32	0.23
100	0.54	0.31	0.21
200	0.53	0.29	0.20
300	0.52	0.28	0.19

Different slopes of the t/V vs. V curves for the PM30 and XM300 membranes indicate the differences in the specific resistances of the cakes (specific resistance is proportional to the slope of the t/V vs. V curve). This mirrors the effect of the membrane type on the characteristics of the cake layer reported by Fane et al. [20]. The XM300 membranes have higher water flux than the PM30 membranes (see Table 1). For a higher initial 'approach velocity', a more open cake with lower specific resistance is formed [21]. This observation

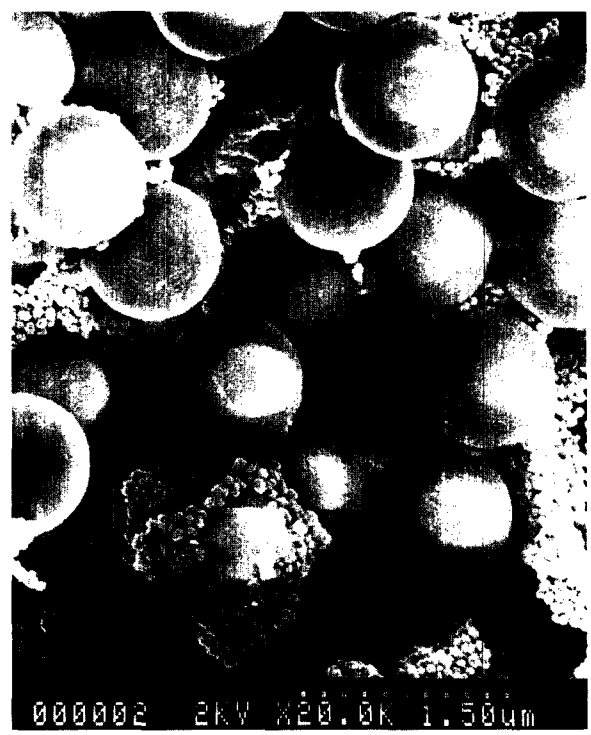

Fig. 9. SEM micrograph of XM300 membrane surface after filtering 800 ml of a mixture of Au sol and latex (10 mg l^{-1} Au, 10 mg l^{-1} latex, 100 kPa, unstirred, pH = 4).

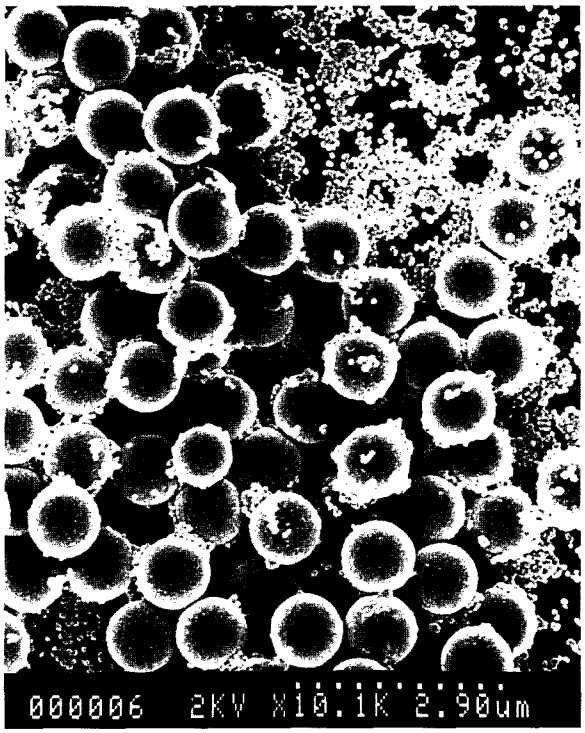

Fig. 10. SEM micrograph of PM30 membrane surface after filtering 100 ml of a mixture of Au sol and latex (10 mg l^{-1} Au, 10 mg l^{-1} latex, 100 kPa, unstirred, pH = 4).

is similar to that found for the MF of sol-only feed [7]. Another possible explanation is based on membrane hydrophobicity. The XM300 membranes are less hydrophobic than the PM30 membranes. The cake on the XM300 membrane is looser than the cake on the PM30 membrane surface, due to less adsorption of the particles, resulting in lower specific resistance.

3.5. Characteristics of the colloidal mixture cake layer

The specific resistances of Au sol, latex and their mixture which were calculated from the slope of the t/V vs. V curve, are given in Table 4. The calculated specific resistance shows an increase with pressure. The compressibility factor of the mixture of Au sol and latex is 0.33 (Fig. 8); this is higher than the individual compressibility factors of Au sol (0.14) and latex (0.25).

It is evident that the specific resistance of the mixture is significantly higher (more than an order of magnitude) than the individual components. This is due to the filling of the void space between the large latex particles with the much smaller colloidal gold. It is possible to estimate the order of magnitude increase by considering the way the gold cake is altered by the presence of latex. Thus, a given loading of gold has only 0.3 of the volume available (the remainder is taken up by latex particles). This would produce a gold cake $(0.3)^{-1}$ thicker than for gold alone, i.e. 3.3 times thicker. In addition, the pathway through the voids is tortuous, which also increases the path length. Typical tortuosity is 3, so effective 'resistance' increases $3.3 \times 3 \approx 10$ times. This analysis anticipates that α_{Au} (in the mixture) would be ca. $10 \times \alpha_{Au}$ (alone). In practice the specific resistance increase is 13 to 20 times.

The cake porosity, estimated from the Carman–Kozeny equation

$$\alpha = 180(1-\epsilon)/(\rho d_p^2 \epsilon^3) \quad (1)$$

in which α is the cake specific resistance, ϵ is the porosity, ρ is the density and d_p is the particle diameter, is shown in Table 5. The mean diameter for the mixture ($d_p = 65$ nm) is based on mass fractions (Eq. (2).

$$d_p^3 = (\rho_1 n_1 d_1^3 + \rho_2 n_2 d_2^3)/(\rho_1 n_1 + \rho_2 n_2) \quad (2)$$

where ρ is the density, n is the number of particles, d is the diameter of the particles and 1 and 2 refer to the first and second particle in the mixture.

The high porosity in the case of Au sol could be due to the aggregation of the gold particles. Whereas for a monosize packing the porosity is at least 0.3, in a binary mixture the porosity drops due to the filling of the voidage between the larger particles by small ones (Fig. 9). In this work the size ratio was 50 nm/1000 nm, i.e. 0.05. For a binary mixture of size ratio 0.058 Fedors and Landel [22] report a porosity of 0.19; for a size ratio of 0.06 McGeary [23] reports a porosity of 0.16. The porosity of a binary mixture also changes by changing the volume fraction. In this work the volume fraction of latex particles in the mixture is 95% with 5% gold particles. With a volume fraction of 95% for larger particles and a radius ratio of 0.05 or 0.053 (similar to this work) the reported

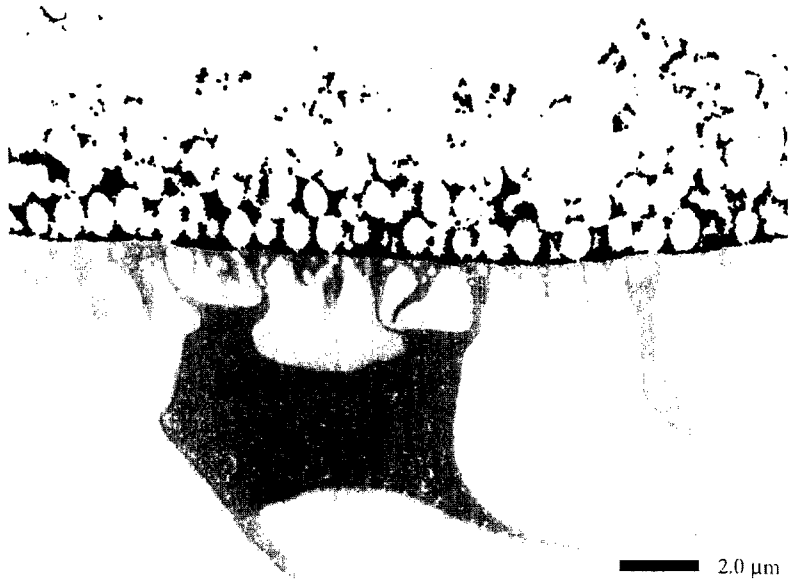

Fig. 11. TEM micrograph of XM300 membrane surface after filtering 800 ml of a mixture of Au sol and latex (10 mg l^{-1} Au, 10 mg l^{-1} latex, 100 kPa, 400 rev min^{-1}, pH = 4).

porosity is 0.34 [23] or 0.32 [22]. For the same volume fraction and a radius ratio less than 0.1 the porosity is reported as 0.32 [24].

The calculated porosity shows a decrease with increasing transmembrane pressure: this is due to the effect of pressure, causing more dense layers than the random packing by gravity.

Owing to the formation of several layers of latex particles on the membrane surface that are surrounded with gold particles (Figs. 10 and 11), the cake thickness is estimated to be between 1 and 10 μm, depending on the permeate volume and the applied transmembrane pressure.

4. Conclusions

The ultrafiltration behaviour of very dilute (ca. 10 ppm) mixtures of gold (50 nm) and latex (1 μm) colloidal suspensions has been investigated for a range of conditions (varying transmembrane pressure, pH and stirring) in a batch cell with PM30 and XM300 ultrafiltration membranes.

Both types of membrane gave higher flux and lower retention for increasing ΔP or pH. The retention was essentially complete for the PM30 membrane. For ultrafiltration membranes a lower pressure produced slower flux decline, lower solute resistance and higher retention.

The prevailing mechanism was cake formation during the course of ultrafiltration. However, pore plugging can occur in ultrafiltration if the membrane pores are comparable in size with the particles.

The measured cake specific resistance showed an increase with pressure. The cake porosity was smaller than the reported porosity for the random packing of a binary mixture due to the effect of applied pressure.

References

[1] I. Matsuo, Novel ultrafiltration module as a final filter in the ultrapure water system, Proc. Annu. Semiconductor Pure Water Conf., Santa Clara, CA, USA, 1991, pp. 108–127.

[2] R. Gerard, R. Lesan, I. Kawada, K. Tasaka, Role of membrane equipment in state-of-the-art ultrapure water systems, Proc. Annu. Semiconductor Pure Water Conf., Santa Clara, CA, USA, 1991, pp. 69–86.

[3] J.G. Jacangelo, J.M. Laine, K.E. Carns, E.W. Cummings, J. Mallevialle, Low-pressure membrane filtration for

removing Giardia and microbial indicators, Am. Water Works Assoc. J. 83 (9) (1991) 97–106.
[4] C. Cabassud, C. Anselme, J.L. Bersillon, P. Aptel, Ultrafiltration as a nonpolluting alternative to traditional clarification in water treatment, Filtr. Sep. 28 (3) (1991) 194–198.
[5] E.A. Bicknel, D.M. Dziewulski, L.S. Sturman, G. Belfort, Concentration of seeded and naturally occurring enteroviruses from waters of varying quality by hollow fibre ultrafiltration, Water Sci. Technol. 17 (1985) 47–62.
[6] N. Ratanmohan, R. Garretson, L.G. Irving, An ultrafiltration system for the recovery of viruses in effluent, Aust. J. Med. Lab. Sci. 1 (1980) 149–154.
[7] K.J. Kim, S.S. Madaeni, V. Chen, A.G. Fane, The microfiltration of very dilute colloidal suspensions, J. Colloid Interface Sci. 166 (1994) 462–471.
[8] S.S. Madaeni, A.G. Fane, Microfiltration of very dilute colloidal mixtures, J. Membr. Sci. 113 (1996) 301–312.
[9] J. Turkevich, P.C. Stevenson, J. Hiller, A study of the nucleation and growth processes in the synthesis of colloidal gold, Discuss. Faraday Soc. 11 (1951) 55–75.
[10] G. Frens, Controlled nucleation for the regulation of the particle size in monodisperse gold suspensions, Nature Phys. Sci. 241 (1973) 20–22.
[11] K.J. Kim, A.G. Fane, C.J.D. Fell, Quantitative microscopic study of surface characteristics of ultrafiltration membranes, J. Membr. Sci. 54 (1990) 89–102.
[12] M.-S. Lee, H. Yamasaki, T. Tanaka, K. Nakanishi, Crossflow membrane filtration of highly viscous microbial broth, Proc. Asia–Pacific Biochemical Engineering Conf., Yokohama, Japan, 1992, pp. 529–532.
[13] AWWA Membrane Technology Research Committee, Committee report: membrane processes in potable water treatment, J. Am. Water Works Assoc. 84 (1992) 59–67.
[14] R.M. McDonogh, Ultrafiltration of colloids, Ph.D. Thesis, University of New South Wales, 1987.
[15] K.J. Kim, A.G. Fane, M. Nyström, A. Pihlajamaki, R.W. Bowen, H. Mukhtar, Evaluation of electroosmosis and streaming potential for measurement of electric charges of polymeric membranes, J. Membr. Sci. 116 (1996) 149–159.
[16] M. Nyström, M. Lindstrom, E. Matthiasson, Streaming potential as a tool in the characterisation of ultrafiltration membranes, Colloids Surf. 36 (1989) 297–312.
[17] J. Hermia, Constant pressure blocking filtration laws, Trans. Inst. Chem. Eng. 60 (1982) 183–187.
[18] T.B. Choe, P. Masse, A. Verdier, M.J. Clifton, Flux decline in batch ultrafiltration: concentration polarisation and cake formation, J. Membr. Sci. 28 (1986) 1–15.
[19] T. Murase, E. Iritani, J.H. Cho, M. Shirato, Determination of filtration characteristics of power-law non-Newtonian fluids—solids mixtures under constant-pressure conditions, J. Chem. Eng. Jpn. 22 (1) (1989) 65–71.
[20] A.G. Fane, P.H. Hodgson, G.L. Leslie, Crossflow microfiltration of biofluids and biomass—new perspectives, Proc. 6th World Filtration Congress, Nagoya, Japan, 1993, pp. 5–13.
[21] A. Rushton, M. Hosseini, I. Hassan, The effects of velocity and concentration on filter cake resistance, J. Sep. Process Technol. 1 (3) (1980) 35–41.
[22] R.F. Fedors, R.F. Landel, An empirical method of estimating the void fraction in mixtures of uniform particles of different size, Powder Technol. 23 (1979) 225–231.
[23] R.K. McGeary, Mechanical packing of spherical particles, J. Am. Ceram. Soc. 44 (1961) 513–522.
[24] A.B. Yu, N. Standish, Porosity calculations of multi-component mixtures of spherical particles, Powder Technol. 52 (1987) 233–241.